

Original Research

Tumor-associated tissue eosinophilia promotes angiogenesis and metastasis in head and neck squamous cell carcinoma



Tsung-Lun Lee^{a,c,†}; Tien-Hua Chen^{b,c,†};
Ying-Ju Kuo^{c,d}; Hsin-Yi Lan^e; Muh-Hwa Yang^{b,f,g,*};
Pen-Yuan Chu^{a,c,**}

^a Department of Otolaryngology, Taipei Veterans General Hospital, Taipei, Taiwan

^b Division of Medical Oncology, Department of Oncology, Taipei Veterans General Hospital, Taipei, Taiwan

^c Faculty of Medicine, National Yang Ming Chiao Tung University, Taipei, Taiwan

^d Department of Pathology, Taipei Veterans General Hospital, Taipei, Taiwan

^e Department of Biotechnology and Laboratory Science in Medicine, National Yang Ming Chiao Tung University, Taipei, Taiwan

^f Institute of Clinical Medicine, National Yang Ming Chiao Tung University, Taipei, Taiwan

^g Cancer Progression Research Center, National Yang Ming Chiao Tung University, Taipei, Taiwan

Abstract

Eosinophils are terminally differentiated leukocytes that participate in the process of chronic inflammation and allergy and are able to release multiple cytokines into the surrounding tissue environment. Tumor-associated tissue eosinophilia (TATE) is the presence of eosinophils in the tumor or in the neighboring stroma and has been observed in various types of cancer. In head and neck squamous cell carcinoma (HNSCC), the clinical relevance of TATE has not been concluded yet because of the inconsistent results in different studies. In our study, we focus on the prognostic effects of TATE on HNSCC and how TATE can influence tumor behavior and tumor microenvironment. We first showed that in both the TCGA-HNSC cohort and our cohort of patients with HNSCC who had received curative surgery, TATE is correlated with worse overall survival. To investigate the underlying mechanism of how TATE leads to poor clinical outcomes, we showed that activated eosinophils produce a variety of cytokines and chemokines, and activated TATE-derived culture medium promotes tumor migration mainly through CCL2. We also showed that eosinophils are capable of inducing angiogenesis and that HNSCC samples enriched with TATE are highly correlated with tumor angiogenesis. Furthermore, HNSCC enriched with TATE had more aggressive pathological features, including regional lymph node metastasis, perineural invasion, lymphovascular invasion, and tumor growth. Lastly, we showed that HNSCC enriched with TATE is associated with immunosuppressive tumor microenvironment. Taken together, our results suggest that TATE promotes cancer metastasis and angiogenesis which results in a poor clinical outcomes in HNSCC.

Neoplasia (2023) 35, 100855

Keywords: Tumor-associated tissue eosinophilia, Head and neck squamous cell carcinoma, Angiogenesis, Metastasis

Abbreviations: GSEA, Gene set enrichment analysis; HNSCC, Head and neck squamous cell carcinoma; LVI, lymphovascular invasion; PNI, perineural invasion; TATE, Tumor-associated tissue eosinophilia; TCGA-HNSC, The Cancer Genome Atlas Head-Neck Squamous Cell Carcinoma; TILs, tumor-infiltrated lymphocytes; TVGH, Taipei Veterans General Hospital.

* Corresponding author: Institute of Clinical Medicine, National Yang Ming Chiao Tung University, Taipei 112, Taiwan.

** Co-corresponding author: Department of Otolaryngology, Taipei Veterans General Hospital, Taipei 112, Taiwan.

E-mail addresses: mhyang2@nycu.edu.tw (M.-H. Yang), pychu@vghtpe.gov.tw (P.-Y. Chu).

[†] The first two authors contributed equally to this work.

Received 4 July 2022; accepted 8 November 2022

Introduction

The standard of care for locally advanced head and neck squamous cell carcinoma (HNSCC) includes surgical resection of the operable tumor followed by adjuvant treatment or primary chemoradiation (CCRT) [1]. For those who had received surgical resection, several pathological features are correlated with a higher risk of recurrence and distant metastasis and indicate

potential needs for adjuvant CCRT. These pathologic features include major risk factors: extranodal extension and surgical margin involved, and minor risk factors: perineural invasion (PNI), lymphovascular invasion (LVI), large primary tumor (pT3/T4) or extensive lymph node metastasis (pN2/N3) [1–3]. For HNSCC patients who had major pathologic risk factors, adjuvant CCRT can effectively decrease the risk of recurrence and prolong survival [4]. However, there is still a significant proportion of patients who suffer from recurrence and poor clinical outcomes for those without identifiable risk characteristics. Therefore, it is of utmost importance to identify additional pathologic risk characteristics for the recurrence of HNSCC.

Eosinophils are terminally differentiated leukocytes that reside mainly in submucosal tissues and constitute a small proportion of peripheral blood cells [5]. The morphologic hallmark of eosinophils is the abundant cytoplasmic granules, which contain four major proteins: major basic protein (MBP), eosinophil-derived neurotoxin (EDN), eosinophil cationic protein (ECP), and eosinophil peroxidase (EPO), and these four major proteins participate in the eosinophils' activity against helminthic parasites and the mechanism of allergic reaction [5,6]. Aside from these cationic proteins in cytoplasmic granules, eosinophils also exert its activity through cytokine release. Cytokine production of granulocyte-macrophage colony-stimulating factor (GM-CSF), interleukin (IL)-3, and IL-5 by activated eosinophils exert autocrine growth factor activities [7]. Other cytokine production by activated eosinophils includes IL-1 α , IL-6, IL-8, and tumor necrosis factor (TNF)- α , which participate in acute and chronic inflammation, and transforming growth factor (TGF)- α , c-kit ligand stem cell factor (SCF), and TGF- β , which facilitate nearby epithelial hyperplasia and fibrosis [8–13].

Tumor-associated tissue eosinophilia (TATE) is the presence of eosinophils infiltrative into solid tumors or aggregates in the surrounding stroma [14]. TATE is characteristic of Hodgkin's lymphoma, but can also be found in various types of solid cancer, including colorectal cancer, esophageal cancer, cervical cancer, bladder cancer, gastric cancer, and HNSCC [15]. Efforts to elucidate how TATE affects the prognosis of HNSCC showed variable results. Several studies showed beneficial effects of the presence of TATE in HNSCC [14,16,17]. However, more studies showed that TATE was associated with occult lymph node metastasis, stromal invasion, increased tumor size, and poor survival outcomes [18–21]. The underlying mechanism of how eosinophils interact with nearby immune and cancer cells and how eosinophil-derived cytokines affect the surrounding tumor microenvironment remains to be explored. In this study, we investigated the pathological characteristics and survival outcomes in TATE-positive and TATE-negative HNSCC patients, and the underlying mechanism of how activated TATE facilitates angiogenesis and cancer cell migration.

Materials and methods

Study population

The study was approved by the Institutional Review Boards (IRB) of Taipei Veterans General Hospital (TVGH). Two independent set of HNSCC patient samples were used in this study. The first group for immunohistochemistry (IHC) analysis comprised 60 samples from HNSCC patients who received curative surgical treatment in TVGH from October 2017 to June 2020. Patient characteristics (age, sex, exposure to smoking / alcohol / betel nuts, primary tumor location, clinical staging, combined treatment modality) and pathology characteristics (pathology staging, differentiation, perineural invasion, lymphovascular invasion, lymphocytic infiltration, eosinophilic infiltration, tumor growth, tumor emboli, worst pattern of invasion-5 (WPOI-5), extranodal extension) were documented. The second for RNA sequencing comprised frozen samples of 65 dissected tumors derived from 23 HNSCC patients and contralateral normal oral epithelia. The clinical characteristics of the 23 HNSCC patients is illustrated in Supplementary Table 1.

Histopathology evaluation, immunohistochemistry and quantification of IHC Images

For evaluation of TATE in HNSCC samples, hematoxylin and eosin (H&E) counter staining was performed on formalin-fixed paraffin-embedded (FFPE) HNSCC specimens. Enriched with TATE or not was evaluated by a pathologist. Evident TATE infiltration under low power field (LPF, 40X) was defined as TATE-enriched, and scarce or absence of TATE infiltration under LPF was defined as TATE-poor. For evaluation of the vascularization of the tumor samples, IHC for examining the expression of CD31 was performed. Briefly, the FFPE samples were manipulated by deparaffinization, rehydration, epitope retrieval, peroxidase inactivation, and nonspecific protein binding block. The prepared specimen was then stained with anti-CD31 antibody (1:200, catalogue no. 250590, AbbiotecTM, Escondido, CA), followed by Polymer-anti-rabbit Poly-HRP-IgG (catalogue no. RE7140-K, NovolinkTM, Chino,CA) staining. The specimen was visualized by 3,3'-Diaminobenzidine (catalogue no. RE7140-K, NovolinkTM, Chino,CA) chromogen and nuclear staining with hematoxylin, and the slides were scanned with the Vectra Polaris Automated Quantitative Pathology Imaging System (Akoya Bioscience, Marlborough,MA). The percentage of CD31 positive area and the number of blood vessels per region of interest (ROI) were automatically calculated by the inForm Image Analysis System (Caliper LifeSciences, Hopkinton,MA).

Butyric acid-induced eosinophilic differentiation

The subline of human promyelocytic leukemia cell line HL-60, HL-60 clone 15, which harbors capability for eosinophil differentiation, were used in this study. The HL-60 clone 15 cells were maintained in RPMI-1640 medium (catalogue no. 11875093, ThermoFisher Scientific, Waltham,MA), which were supplemented with 10% fetal bovine serum (FBS) (catalogue no. SH30070.03, Cytiva, Marlborough,MA). Both cell lines were cultured at a concentration of 0.5×10^6 cells per milliliter, and then incubated with 0.5 mM butyric acid (catalogue no. B103500, Sigma-Aldrich, St. Louis, Missouri) for 5 days for induction of eosinophilic differentiation [22]. For eosinophil activation, differentiated eosinophils were further incubated with 0.1 μ M elastase (catalogue no. SE563, Elastin Products Company, Owensville,MO) and 50ng/ mL cathepsin G (catalogue no. C4428, Sigma-Aldrich, St. Louis, MO) for 48 hours [23]. After eosinophil activation, cells were kept in serum-free medium for 48 hours and then conditioned medium was collected.

Cytokine array, HUVEC tube formation assay, migration assay and immunofluorescence

These assays were performed as previously described [24–26]. Simply put, detection of eosinophil-derived cytokines was performed by Human Cytokine Array (catalogue no. C5, RayBiotech, Peachtree Corners,GA). The array was conducted sequentially by blocking, incubation overnight with conditioned medium, biotinylated antibody cocktail incubation, HRP- streptavidin incubation, and then chemiluminescence detection. The intensity of each well was quantified by ImageJ software. For HUVEC tube formation assay, 5×10^4 HUVEC cells were added to the 1:1 Matrigel medium mixture and conditioned medium from M0 macrophages, M2 macrophages, or eosinophils were added. The plate was then incubated at 37°C for 48 hours and the images were captured by inverted microscopy (Olympus CKX41, Olympus Corporation, Tokyo, Japan). The number of tube formation and junctions was quantified and analyzed. For Boyden chamber migration assay, 0.5×10^4 cells of the HNSCC cell line FADU or OECM-1 cells were suspended in FBS-free medium and plated in the upper chamber. Culture medium with 10% FBS was added to the lower chamber. After 24 hours of incubation, the cells left in the upper

chamber were removed. Cells migrated to the lower surface of the membrane were fixed in 4% formaldehyde and stained with Coomassie Brilliant Blue (catalogue no. AF-279-NA, R&D Systems, Minneapolis, MN). The number of migrated cells was quantified under a 40X objective lens in 5 different fields for each sample. For immunofluorescence, cells were sequentially fixed with 4% formaldehyde, permeated with Triton-X 100, blocked for 1 hour and incubated with anti-human Siglec-8 antibody (catalogue no. 130-098-716, Miltenyi Biotec, Bergisch Gladbach, Germany). FITC-conjugated goat antimouse IgG (catalogue no. F-2761, ThermoFisher Scientific, Waltham, MA) was used to visualize Siglec-8 signals and the cell nuclei were counterstained with Hoechst 33342. The prepared immunofluorescent slides were then scanned by a Leica laser scanning confocal microscope.

Precipitation of trichloroacetic acid (TCA) protein and western blot

For protein collection from conditioned medium, samples were mixed with 100% TCA (catalogue no. T0699, Sigma-Aldrich, St. Louis, MO) in a 1:4 ratio. After resting at 4°C for 10 minutes, the samples were centrifuged at 14,000 rpm for 5 minutes. The pellets were washed with acetone and boiled in sample buffer at 95°C. The prepared sample was loaded onto SDS-PAGE for western blot as previously described [24–26].

Multiplex immunofluorescence

Multiplex immunofluorescence was performed on HNSCC samples enriched with or lacking TATE. After initial deparaffinization, rehydration, and epitope retrieval, pathology slides were managed with Opal Polaris 7 Color IHC Detection Kits (catalogue no. NEL861001KT, Akoya Bioscience, Marlborough, MA). Seven cycles of repetitive steps (blocking, primary antibody incubation, incubation with opal polymer HRP, and signal amplification) were performed on each slide for detection of multiple target proteins. The panel includes markers for tumor-infiltrative lymphocytes (TILs): CD4 (catalogue no. MA5-12259, ThermoFisher Scientific, Waltham, MA), CD39 (catalogue no. ab223842, abcam, Cambridge, UK), CD8a (catalogue no. MA5-13473, ThermoFisher Scientific, Waltham, MA), TIM-3 (catalogue no. 45208, Cell Signaling Technology, Danvers, MA), FOXP3 (catalogue no. 12-4777-42, ThermoFisher Scientific, Waltham, MA), PD1 (catalogue no. ab137132, abcam, Cambridge, UK), GMZB (catalogue no. 46890, Cell Signaling Technology, Danvers, MA). Subsequently, the slides were incubated with PanCK antibody (catalogue no. 27988, abcam, Cambridge, UK) and nuclei staining with DAPI. The prepared slides were scanned by the Vectra Polaris Automated Quantitative Pathology Imaging System (Akoya Bioscience, Marlborough, MA) and analyzed by the inForm Image Analysis System (Caliper LifeSciences, Hopkinton, MA).

Gene set enrichment analysis (GSEA) and TIMER2.0 analysis

Sixty-five HNSCC samples from 23 patients of the TVGH cohort were subjected to RNA sequencing analysis. Sample RNA was extracted with TRIzol reagent (catalogue no. 15596026, Invitrogen™, Carlsbad, CA) and 1 µg of RNA was applied to the Illumina TruSeq RNA Sample Prep Kit (Illumina, San Diego, CA). After reverse transcription, sequencing was performed with Illumina NextSeq500 and Illumina HiSeq2500 (Illumina, San Diego, CA). The reads were imported to STAR v2.6.1a and the reference genome GRCh38.94 was used for alignment into BAM files. The BAM files were imported into RSEM v1.3.1, and the expected count tables were acquired from RSEM output gene results files. The log transformation was performed with DESeq2 v1.26.0. The RNA sequencing database was integrated with pathology information on TATE-enriched or TATE-poor, and differentially expressed genes were analyzed using GSEA software with the selection of a collection of signature gene datasets (h.all.v7.5.symbols.gmt) [27]. TIMER2.0 was also used to analyze the

survival difference between the TATE positive and TATE-negative groups from The Cancer Genome Atlas Head-Neck Squamous Cell Carcinoma (TCGA-HNSC) cohort [28,29]. The accession numbers for the data reported in this paper is GSE 181300 (review token: wjuhsswmvnylxub).

Statistics

The Chi-square test and Fisher's exact test were used to test the null hypothesis of categorical variables. The two-sided Mann-Whitney U test was used to compare continuous variables between two groups. The Kaplan-Meier estimate was used for the analysis of survival data and the two-sided log rank test was used to compare the difference in survival between two groups. A P-value lower than 0.05 was considered statistically significant. All statistical analyzes were performed with GraphPad Prism 6 and SPSS version 22.

Results

TATE is associated with aggressive pathologic features and poor clinical outcomes of HNSCC

We first investigated the clinical significance of TATE in TCGA database and our clinical cohort. From the TCGA-HNSC cohort, the patient in the TATE-enriched HNSCC group was associated with an increased risk of death (hazard ratio 1.67, $p < 0.001$) compared to the TATE-poor HNSCC group (Fig. 1A). For the TVGH cohort, a total of 68 HNSCC samples acquired by curative surgery were analyzed for the abundance of TATE, and 8 samples with involved surgical margin were excluded from the survival analysis (Fig. 1B-C). There were no significant differences between TATE-enriched and TATE-poor groups with respect to clinical characteristics, including age, gender, life habits, primary tumor location, clinical stage, and perioperative treatment (Table 1). Survival analyses showed that the overall survival (OS) was significantly better in the TATE-poor group compared to the TATE-enriched group ($p = 0.04$), while recurrence-free survival (RFS) was not significantly different between two groups (Fig. 1D). TATE-enriched samples were also associated with aggressive pathological characteristics including regional lymph node metastasis (63% vs. 25%, $p = 0.003$, Fig. 1E), perineural invasion (74% vs 23%, $p < 0.001$, Fig. 1F), lymphovascular invasion (58% vs 35%, $p = 0.09$, Fig. 1G), tumor budding (95% vs. 42%, $p < 0.001$, Fig. 1H); whereas TATE was not associated with increased size of primary tumor (Fig. 1I).

Activated eosinophils secreted CCL2 promotes migration of HNSCC cells

We next investigated whether activated eosinophils promote HNSCC migration. We firstly established the in vitro activated eosinophils. The schema is illustrated in Fig. 2A. With butyric acid treatment, cells of the HL-60 clone 15 (HC15) successfully differentiated to eosinophils (Fig. 2B). The HC15-derived eosinophils were then activated by elastase and cathepsin G and conditioned medium was collected after changing to serum-free medium for 48 hours. Immunofluorescence of siglec-8 confirmed successful activation of the differentiated eosinophils (Fig. 2C). Next, we analyzed the upregulated cytokines/chemokines in activated eosinophils compared to the untreated HC15 cells by the Human Cytokine Array. A series of cytokines and chemokines were elevated in activated eosinophils, including IL-1 β , IL-2, IL-12, CCL2, CCL11, CCL17, IFN γ , TGF β 1, and PDGF β (Fig. 2D-E). The elevated level of CCL2 in activated eosinophil-derived conditioned medium was confirmed by western blot (Fig. 2F).

We further examined whether CCL2 is responsible for the induction of HNSCC migration. The HNSCC cell lines FADU and OECM-1 cells were incubated with the conditioned media harvested from activated eosinophils. A significantly increased number of migrated tumor cells

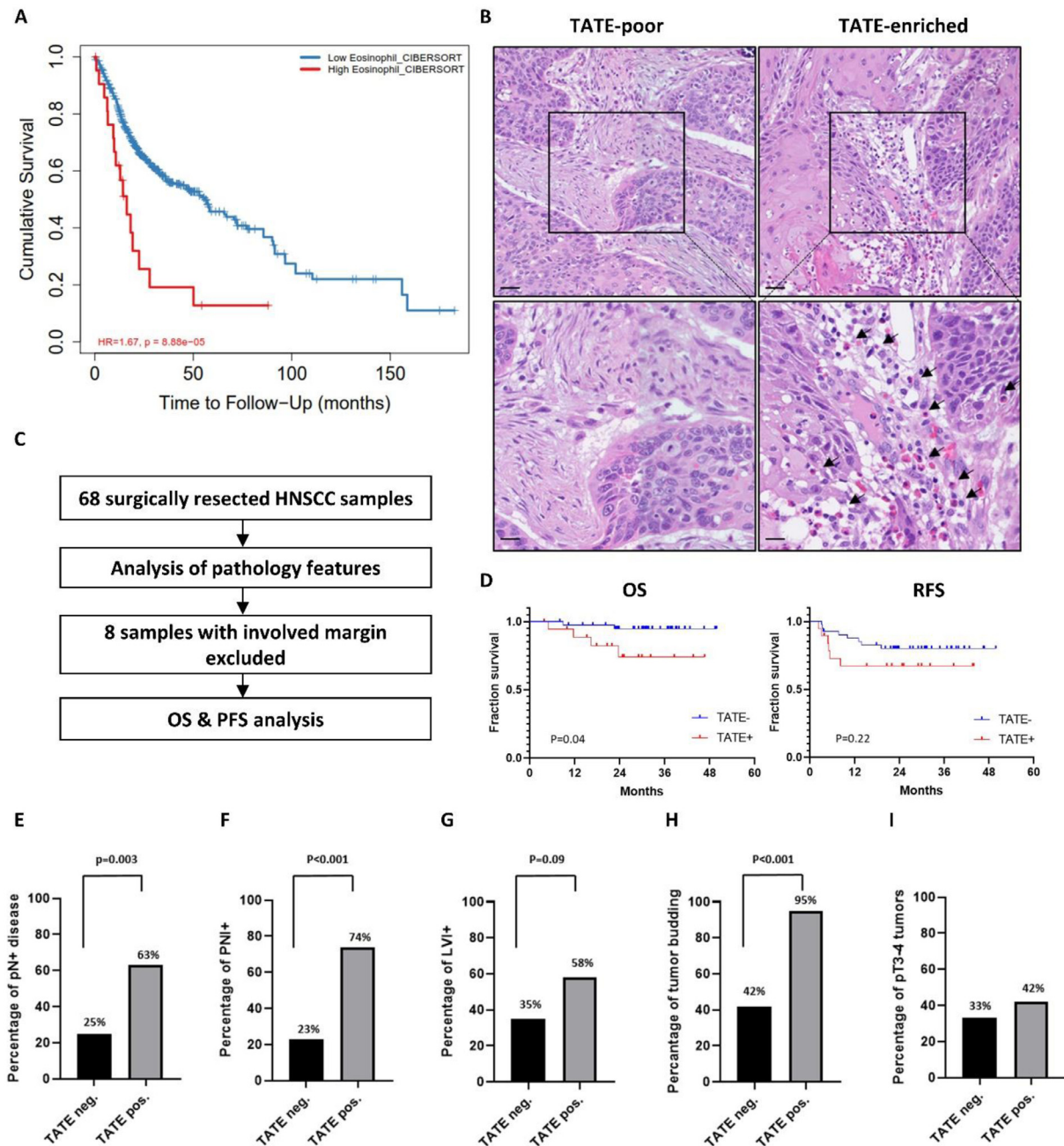


Fig. 1. TATE is correlated with poor pathological characteristics and survival outcomes in HNSCC. **A**, TIMER2.0 analysis of the survival difference between the TATE-enriched and TATE-poor groups from TCGA-HNSCC cohort. **B**, Representative H&E staining of TATE-enriched (right) and TATE-poor (left) HNSCC specimen from TVGH cohort. Scale bar: upper, 50µm; lower, 20µm. Black arrow: eosinophil. **C**, HNSCC patients who received curative surgery in TVGH were screened (n=68), and patients with surgical margin free of malignant cells were enrolled for survival analysis (n=60). **D**, Kaplan-Meier survival plot of OS and RFS for TVGH cohort. **E-I**, Evaluation of poor pathological features. pN+: lymph node metastasis, PNI: perineural invasion, LVI: lymphovascular invasion.

was noted in the conditional media-treated HNSCC cells. Neutralization of CCL2 by the anti-CCL2 antibody abrogated the conditional media-induced HNSCC migration (Fig. 3A-B). Because CCL2 has been noted to induce epithelial-mesenchymal transition (EMT) in oral squamous cell carcinoma [30], we examined the correlation between TATE and EMT signature in TVGH HNSCC database. The result showed that TATE was associated with the EMT signature in HNSCC (Fig. 3C). The above results indicate that activated eosinophils promote HNSCC migration through CCL2.

TATE induces angiogenesis in HNSCC

We next examined whether TATE is able to induce angiogenesis in HNSCC. To achieve this goal, HUVEC tube formation assay was applied. We treated HUVEC with conditioned media from M0 macrophages (a baseline control), M2 macrophages (a positive control), and activated eosinophils. A significantly increased number of enclosed spaces and junctions was observed when treated with conditioned media derived from M2 macrophages activated eosinophils (Fig. 4A-B). We further examined

Table 1

Clinical characteristics and correlation to TATE in 60 analyzed HNSCC cases.

	With TATE (%) (n=19)	Without TATE (%) (n=41)	p-value
Age y/o (95% CI)	52.4 (48.2-56.5)	55.8 (52.8-58.9)	0.285
Sex			
Male	17 (89.5)	38 (92.7)	0.933
Female	2 (10.5)	3 (7.3)	
Tobacco use			
Yes	16 (84.2)	36 (87.8)	0.978
No	3 (15.8)	5 (12.2)	
Alcohol use			
Yes	12 (63.2)	24 (58.5)	0.734
No	7 (36.8)	17 (41.5)	
Betel nuts use			
Yes	14 (73.7)	20 (48.8)	0.070
No	5 (26.3)	21 (51.2)	
Primary tumor location			
Oral cavity	17 (89.5)	39 (95.1)	0.071
Oropharynx	0 (0.0)	2 (4.9)	
Hypopharynx	2 (10.5)	0 (0.0)	
Clinical, T			
cT1/ cT2	14 (73.7)	27 (65.9)	0.140
cT3	3 (15.8)	2 (4.9)	
cT4	2 (10.5)	12 (29.2)	
Clinical, N			
cN0	11 (57.9)	26 (63.4)	0.488
cN1	3 (15.8)	6 (14.6)	
cN2	5 (26.3)	6 (14.6)	
cN3	0 (0.0)	3 (7.4)	
Clinical, stage (AJCC 8th)			
I/ II	9 (47.4)	20 (48.8)	0.811
III	4 (21.5)	6 (14.6)	
IVA/ IVB	6 (31.6)	15 (36.6)	
Induction chemotherapy			
Yes	1 (5.2)	6 (14.6)	0.536
No	18 (94.8)	35 (85.4)	
Adjuvant RT/ CRT			
Yes	11 (57.9)	16 (39.0)	0.172
No	8 (42.1)	25 (61.0)	

y/o: year old; AJCC, The American Joint Committee on Cancer; RT: radiation therapy; CRT: chemoradiation therapy

the correlation between TATE enrichment and angiogenesis in HNSCC by staining CD31 and calculating the CD31-positive area and vascular density in the samples. The pathology of the HNSCC samples was grouped into a TATE enriched area (TATE > 50/ field or TATE 11-49/ field) and a TATE low area (TATE < 10/ field). Significantly increased CD31 positive area and vessel densities were observed in the TATE-enriched area compared to the TATE-low area (Fig. 4C-E). Furthermore, we applied GSEA to analyze the correlation between the existence of TATE and angiogenesis signature in the TVGH HNSCC RNA sequencing database. A significant correlation between TATE and angiogenesis was shown (Figs. 4F). Altogether, our results suggest that TATE promotes angiogenesis in HNSCC.

TATE is associated with infiltration of immunosuppressive T cells in HNSCC

Finally, we investigated the association between TATE and infiltrated immune cells in HNSCC samples. Multiplex immunofluorescence was applied to investigate the correlation between TATE and tumor-infiltrated lymphocytes (TILs) (Fig. 5A-C). All ROIs were divided into three groups

according to the relationship between TATE and all cells in the neighboring stroma (TATE/ stromal cells: TATE-high, > 5%; TATE-medium, 1%-5%, TATE-low, < 1%). The percentage of specific subtype of lymphocytes to total lymphocytes in each ROI was calculated. For the CD4+ cells, the proportions of CD4+, CD4+Foxp3+, CD4+PD1+, and CD4+TIM3+ lymphocytes increased significantly in the TATE-high fields compared to the TATE-low fields (Fig. 5D-G). Regarding the CD8+ cells, the proportion of CD8+ lymphocytes decreased in the TATE high fields, while the proportion of CD8+PD1+ lymphocytes increased significantly in TATE-high fields compared to the TATE-low fields (Fig. 5H-I). The proportion of CD8+TIM3+ lymphocytes was not significantly different between the groups (Fig. 5J). The result implicates that TATE tends to correlate with the infiltration of immunosuppressive T cells in HNSCC.

Discussion

This study focused on determining the clinical relevance of TATE in HNSCC and how TATE affects the surrounding tumor microenvironment. First, we showed that TATE was correlated with a poor prognosis in HNSCC patients who had received curative surgery. Regarding the potential causes

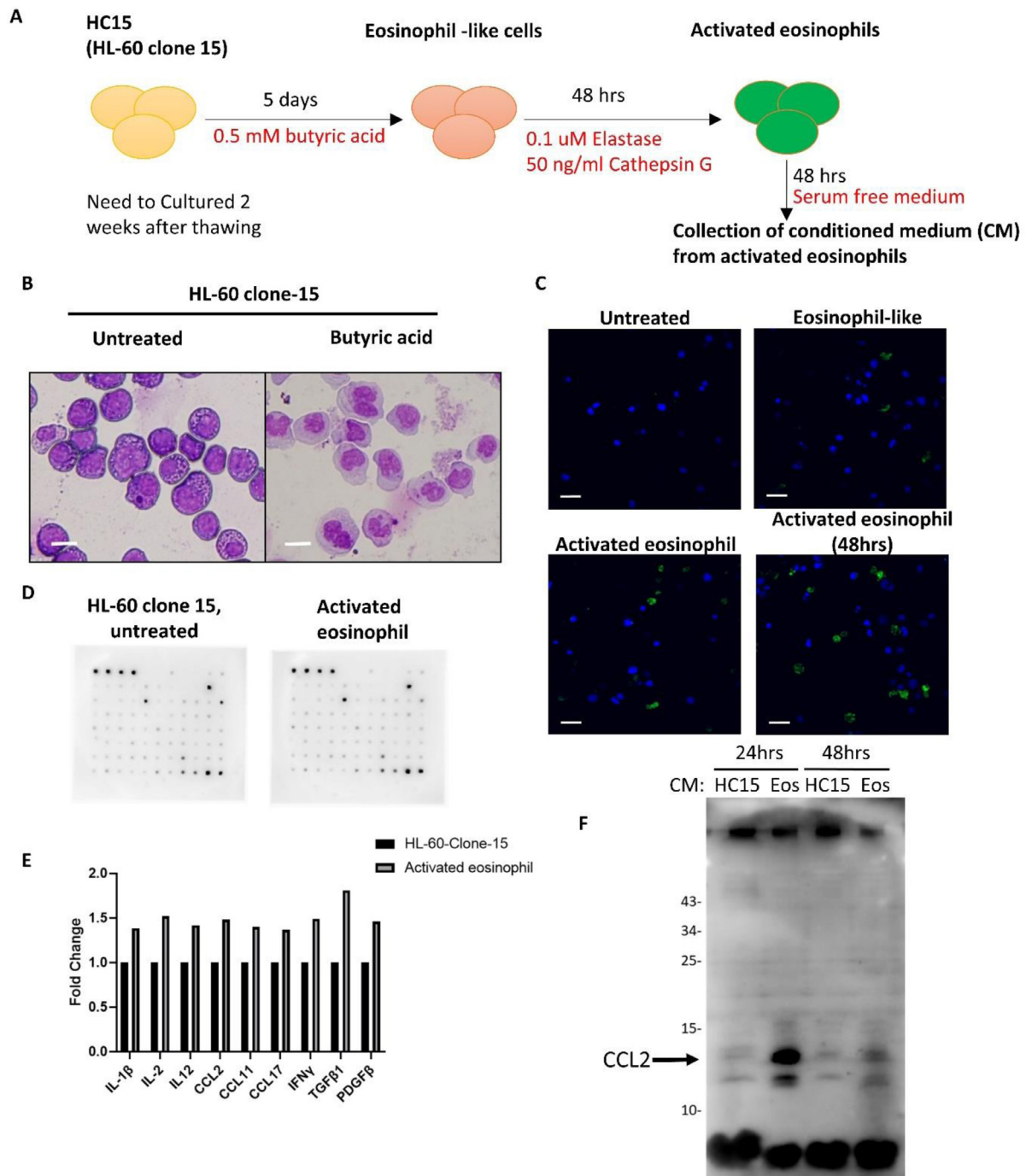


Fig. 2. Establishment of in vitro eosinophil activation model and increased CCL2 release in activated eosinophils. **A**, The schema of butyric acid induced eosinophil differentiation, and activation by elastin and cathepsin G. **B**, Liu's staining of the HL-60 clone 15 (HC15) with or without butyric acid treatment. Scale bar: 10um. **C**, Representative image of immunofluorescent staining of HC15 differentiation into eosinophil and activation. Green: Siglec-8. Blue: DAPI. Scale bar: 10um. **D**, Cytokine array screening of culture medium from untreated HC15 and from activated eosinophils. The list of cytokine/chemokine were documented in **supplementary table 2**. **E**, Image J quantification of cytokine array signal intensity. **F**, TCA precipitation of culture medium from HC15 and eosinophils (Eos) and western blot analysis of CCL-2 protein.

for the correlation between TATE and poor clinical outcomes, we found that TATE was correlated with a higher tumor angiogenesis in clinical specimens. The result is supported by the in vitro assay which showed that activated eosinophils promoted angiogenesis. We also showed that TATE correlated with the EMT signature in HNSCC samples. Furthermore, activated eosinophils increased migration of HNSCC cells which can be

reversed by an anti-CCL2 antibody. Besides, we also showed TATE in HNSCC is correlated with immunosuppressive tumor microenvironment (TME). Importantly, we demonstrated that TATE was correlated with aggressive pathology characteristics which predict a higher risk of distant metastasis. This finding may be attributed to the increased angiogenesis, increased tumor migration, and immunosuppressive TME in HNSCC

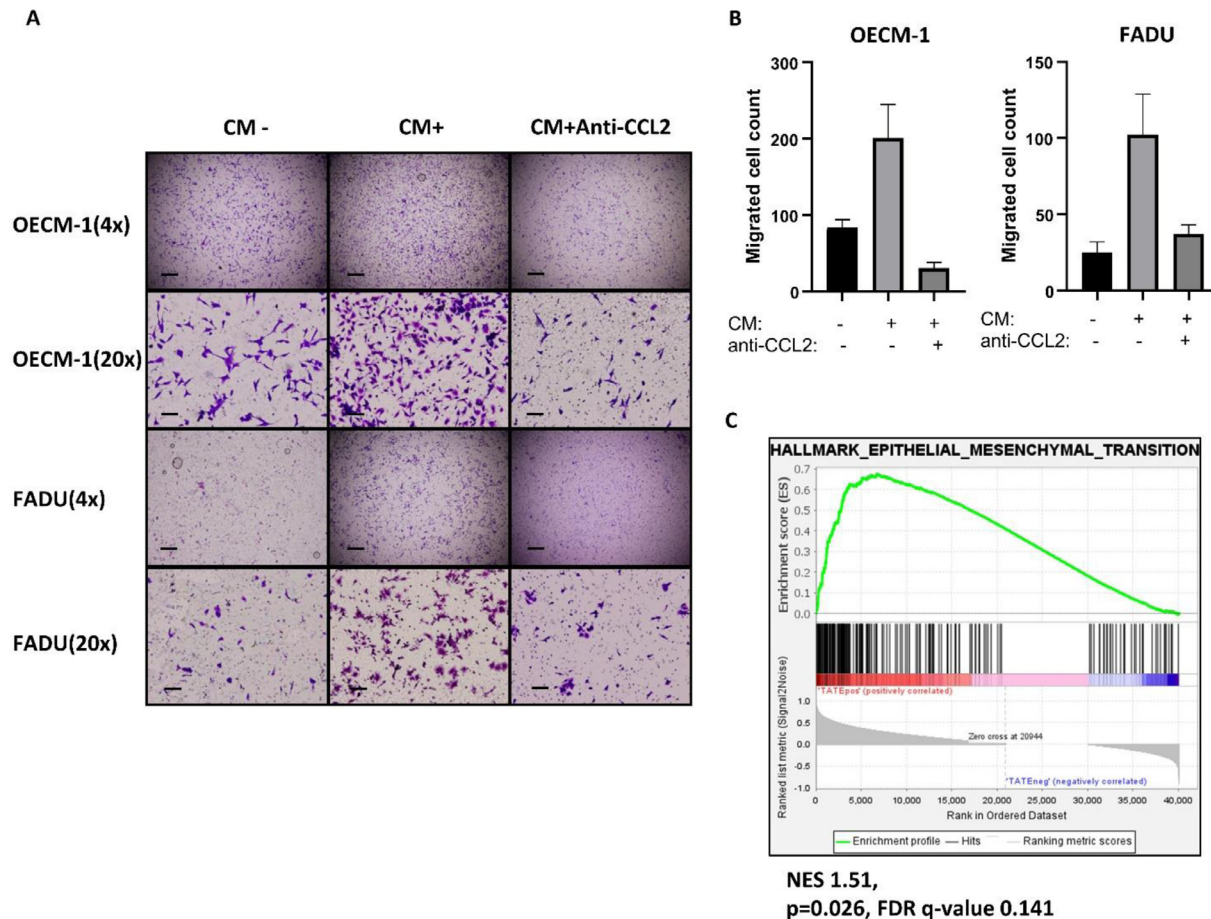


Fig. 3. TATE induces HNSCC metastasis. **A**, migration assay of HNSCC cell lines (OECM-1, FADU), either untreated, treated with conditioned medium (CM), and CM plus Anti-CCL2 antibody. Scale bar: upper, 400um; lower, 80um. **B**, quantification of migrated cells in migration assay. **C**, GSEA analysis of RNA sequencing database from TVGH HNSCC cohort (65 samples from 23 patients) for EMT pathway. NES: normalized enrichment score. FDR: false discovery rate.

enriched with TATE. The abovementioned mechanisms were summarized in Fig. 6.

Previous studies have shown that chronic inflammation promotes carcinogenesis, tumor progression, and metastasis [31]. Eosinophils, a component of immune cells involved in chronic inflammatory conditions such as asthma, had shown in previous studies its ability to mediate the degradation of extracellular matrix through the activation of matrix metalloproteinases (MMP), such as MMP-2, MMP-9, collagenase and stromelysin [32]. Evidence also showed MMP-9 production by eosinophils under activated T cell stimulation and under regulation of stem cell factor (SCF), TGF- β , and TNF- α [32–35]. This release of MMP-9 also facilitates degradation of the basement membrane [36]. Several studies also support the idea that eosinophils induce cancer metastasis through the release of peroxidase and cytokines. In an animal model injected with cells of lung cancer, melanoma, or colorectal cancer, IL5 depletion (the main eosinophil growth factor) decreased the number of lung metastases [37]. This study also showed that eosinophils produce CCL22, which recruit regulatory T cells to the lung and create a prometastatic microenvironment. Another study showed that eosinophil peroxidase facilitates cancer metastasis in a breast cancer model [38]. Recently, a study using mouse models with induced airway inflammation and with induces colitis showed that inflammation-associated eosinophilia increases distant metastasis potential [39]. This study also showed that eosinophils promote tumor migration through CCL6, and blocking the transduction of the CCL6-CCR1 signal can effectively

decrease the potential of distant metastases. In our study, we showed an increased migration ability of HNSCC cancer cells when treated with eosinophil-derived culture medium. Furthermore, we revealed a novel target CCL2 that plays a key role in TATE-facilitated cancer metastasis. CCL2, a chemoattractant for monocytes and basophils, can recruit metastasis-associated macrophages in breast cancer models as shown by prior study [40,41]. Our study also disclosed the relationship of CCL2 with TATE-facilitated cancer metastasis.

Multiple studies had shown that peripheral eosinophils can release angiogenic factors, including VEGF, β -FGF, angiogenin, IL-3, IL-8, and TNF- α , and also induce angiogenesis in asthmatic airways and inflammatory tissues [42–46]. Our study also showed increased angiogenesis in vitro when treated with eosinophil-derived culture medium. Furthermore, we also showed that the TATE-enriched area is associated with elevated angiogenesis activity in HNSCC specimens. All in all, these evidences supported that TATE may induce angiogenesis in HNSCC tumors. Multiple studies had shown that TATE is associated with various aggressive pathological features in HNSCC, including stromal invasion, increased tumor size, advanced stage, and occult neck lymph node metastases [18–21]. These studies also showed lower OS and DFS outcomes in the tumor group enriched with TATE. Our findings in this study also showed that TATE in HNSCC is correlated with regional lymph node metastasis, perineural invasion, lymphovascular invasion, and tumor growth. These characteristics may be a consequence of increased angiogenesis and tumor migration in TATE-enriched HNSCC, and

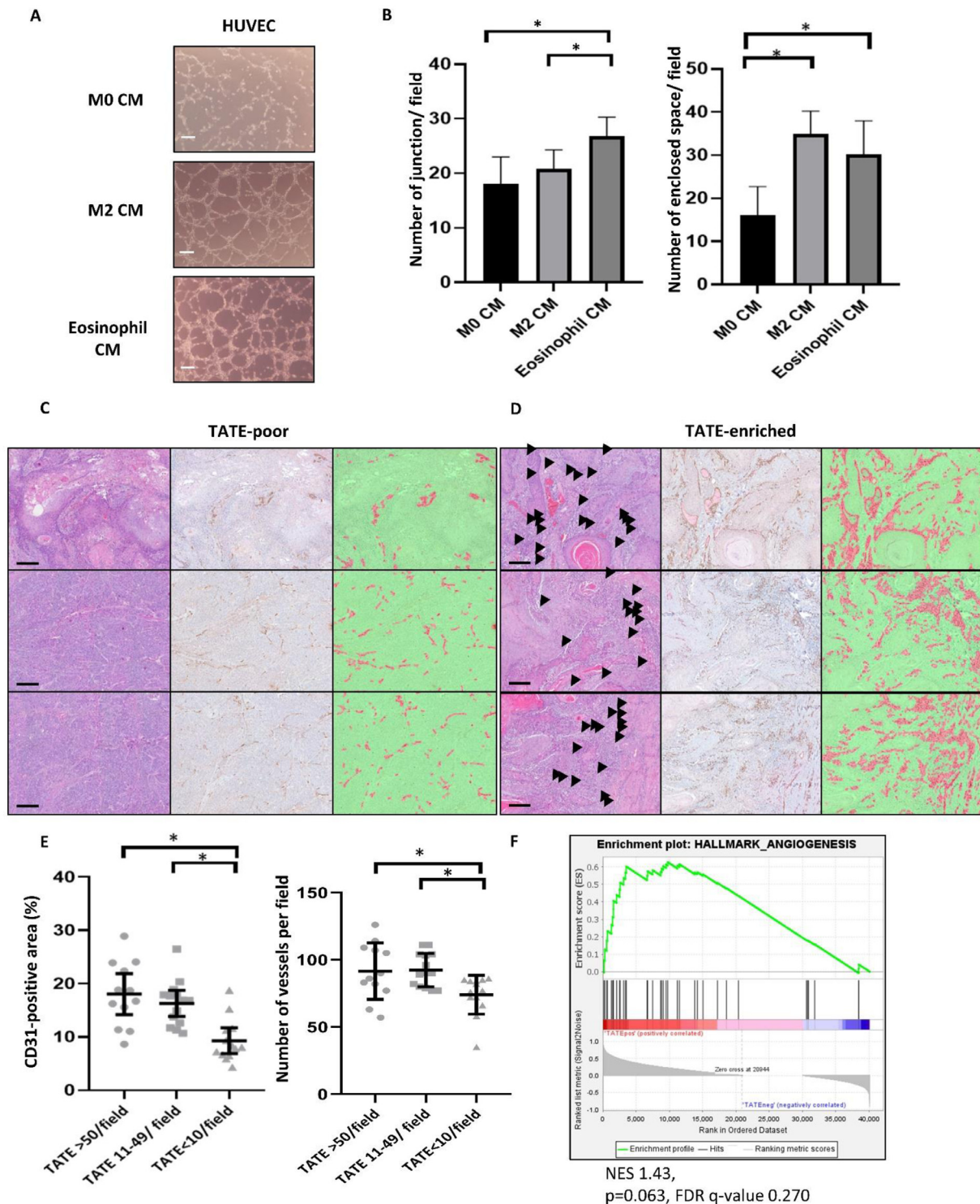


Fig. 4. TATE induces HNSCC metastasis. **A-B**, Culture medium from M0 macrophage (a baseline control), M2 macrophage (a positive control), and activated eosinophil were added to HUVEC assay. Scale bar: 100um. Number of junction and enclosed space were quantified at low power field (40X). Asterisk: $p < 0.05$. **C-E**, Representative images for TATE-poor and TATE-enriched ROI. H&E staining (left), CD31 IHC staining (middle), and automated identification and quantification of CD31-positive area (Right). Scale bar: 200um. Arrowhead: eosinophil. Red area: automatically identified CD31-positive area. Green: automatically identified CD31-negative area. Asterisk: $p < 0.05$. **F**, GSEA analysis of RNA sequencing database from TVGH HNSCC cohort (65 samples from 23 patients) for angiogenesis pathway. NES: normalized enrichment score. FDR: false discovery rate.

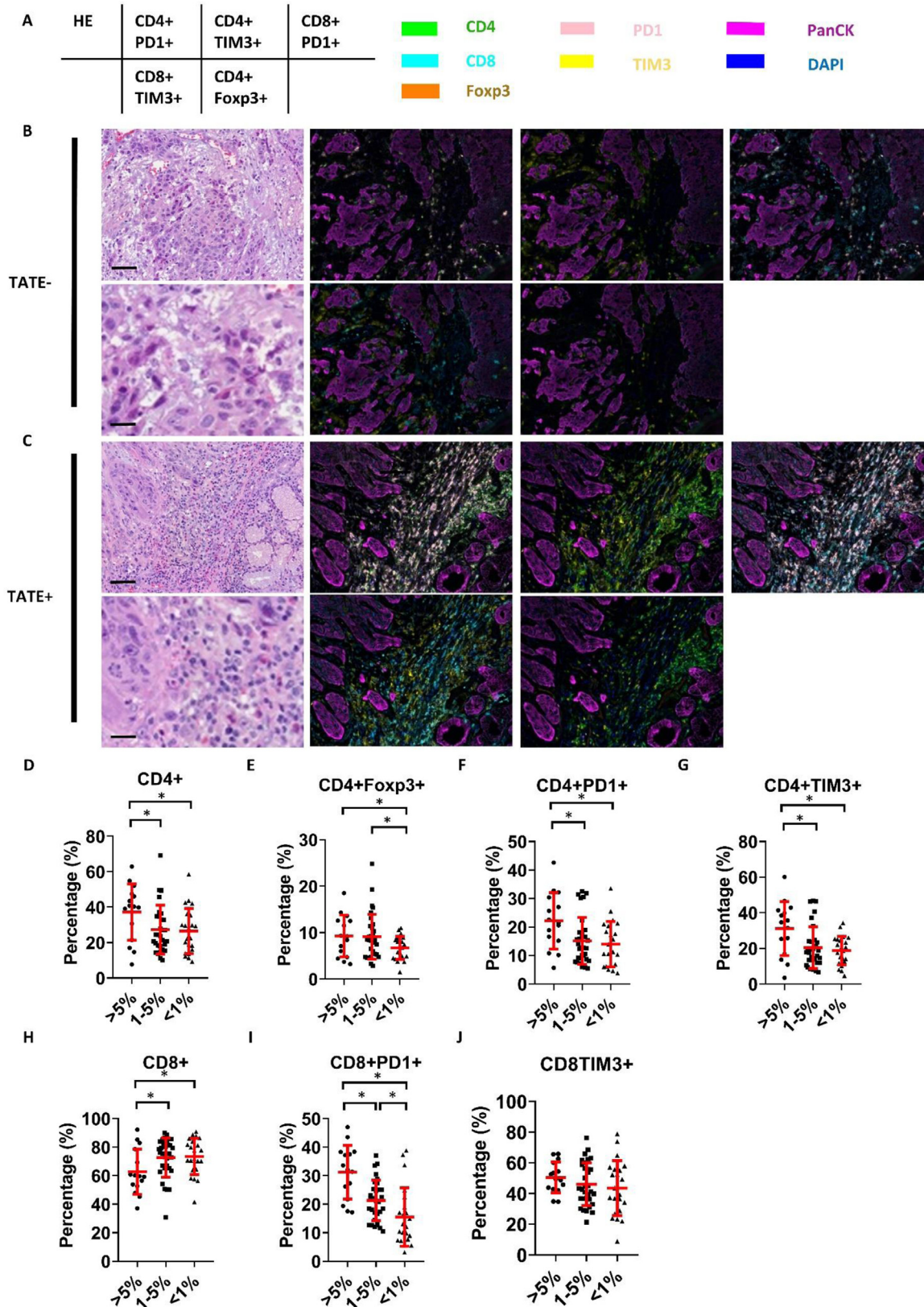


Fig. 5. TATE is associated with infiltration of immunosuppressive T cells in HNSCC. **A**, the list of surface markers in each subgraph. The color of fluorescence for each surface marker was shown on the right side. **B-C**, representative images of multiplex immunofluorescence of surface markers of TILs in TATE-poor and TATE-enriched ROIs. Scale bar: upper, 100um; lower, 20um. **D-J**, automated quantification of percentage of specific component of TILs in total lymphocytes in TATE-enriched (TATE/ stromal cells >5%), TATE-medium (TATE/ stromal cells 1-5%) and in TATE-poor (TATE/ total stromal cells <1%) ROIs. Asterisk: $p < 0.05$.

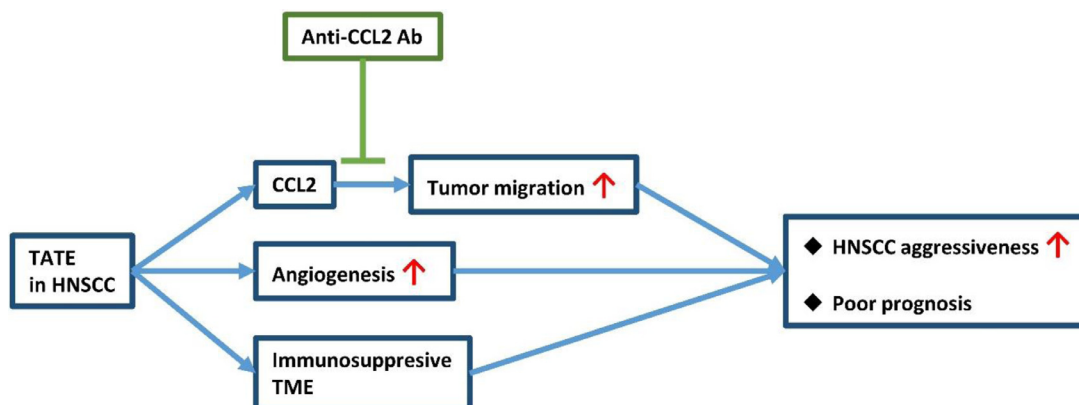


Fig. 6. TATE in HNSCC is correlated with tumor aggressiveness and poor prognosis through multiple mechanisms, which includes CCL2-induced tumor migration, angiogenesis, and immunosuppressive tumor microenvironment (TME).

also predict future locoregional recurrence and distant metastasis. To confirm this hypothesis, we evaluated survival outcomes for the HNSCC patient, and OS is in fact worse in the TATE-enriched group.

This study has several limitations. First, selection bias may exist due to the retrospective nature of this study. Second, the spatial correlation of TATE and increased angiogenesis does not necessarily explain the causality. Third, the effect of TATE depletion on HNSCC metastasis was not tested in this study and remains to be elucidated in a further study. In conclusion, our study suggests that in HNSCC, tumors enriched with TATE are associated with increased angiogenesis, tumor migration, immunosuppressive TME and therefore highly aggressive pathological features and poor clinical outcomes. The clinical and therapeutic implications of TATE in HNSCC warrant further evaluation.

Conclusions

In HNSCC, TATE increased angiogenesis in the tumor part and neighboring tissue, and also increased tumor migration through CCL2 release. TATE also coexisted with immunosuppressive TME. All the mechanisms can lead to increased metastasis, and, indeed, TATE-enriched HNSCC is highly correlated with aggressive pathological features and poor clinical outcomes.

Funding information

This work was supported by grants from the Ministry of Science and Technology (106-2314-B-075-050-MY3 and 109-2314-B-075-013 to Pen-Yuan Chu; 109-2320-B-010-042 and 108-2314-B-010-020-MY3 to Muh-Hwa Yang); the National Health Research Institutes (NHRI-EX109-10919BI to Muh-Hwa Yang); and Featured Areas Research Center Program within the framework of the Higher Education Sprout Project by the Ministry of Education (to Muh-Hwa Yang).

Ethic approval

The study involving human samples was approved by the Institutional Review Board of Taipei Veterans General Hospital (TVGH-IRB certificate No. 2016-04-009C and 2017-03-009C).

Declaration of Competing Interest

The authors declare that no competing financial interests exist with this study.

Supplementary materials

Supplementary material associated with this article can be found, in the online version, at doi:10.1016/j.neo.2022.100855.

CRediT authorship contribution statement

Tsung-Lun Lee: Methodology, Validation, Visualization. **Tien-Hua Chen:** Methodology, Validation, Formal analysis, Data curation, Visualization, Writing – original draft. **Ying-Ju Kuo:** Methodology, Validation, Visualization. **Hsin-Yi Lan:** Methodology, Validation, Formal analysis, Data curation. **Muh-Hwa Yang:** Conceptualization, Investigation, Writing – review & editing, Supervision, Project administration, Funding acquisition. **Pen-Yuan Chu:** Project administration, Funding acquisition, Conceptualization, Investigation.

References

- [1] National Comprehensive Cancer Network. Head and Neck Cancers (Version: 2.2022).
- [2] Cooper JS, Pajak TF, Forastiere AA, et al. Postoperative concurrent radiotherapy and chemotherapy for high-risk squamous-cell carcinoma of the head and neck. *N Engl J Med* 2004;**350**:1937–44.
- [3] Bernier J, Dommenege C, Ozsahin M, et al. Postoperative irradiation with or without concomitant chemotherapy for locally advanced head and neck cancer. *N Engl J Med* 2004;**350**:1945–52.
- [4] Cooper JS, Zhang Q, Pajak TF, et al. Long-term follow-up of the RTOG 9501/intergroup phase III trial: postoperative concurrent radiation therapy and chemotherapy in high-risk squamous cell carcinoma of the head and neck. *Int J Radiat Oncol Biol Phys* 2012;**84**:1198–205.
- [5] Weller PF. Eosinophils: structure and functions. *Curr Opin Immunol* 1994;**6**:85–90.
- [6] Wardlaw AJ, Moqbel R, Barry Kay A. Eosinophils: Biology and Role in Disease. *Adv Immunol* 1995;**60**:151–266.
- [7] Desreumaux P, Janin A, Colombel JF, et al. Interleukin 5 messenger RNA expression by eosinophils in the intestinal mucosa of patients with coeliac disease. *J Exp Med* 1992;**175**:293–6.
- [8] Braun RK, Franchini M, Erard F, et al. Human peripheral blood eosinophils produce and release interleukin-8 on stimulation with calcium ionophore. *Eur J Immunol* 1993;**23**:956–60.
- [9] Costa JJ, Matossian K, Resnick MB, et al. Human eosinophils can express the cytokines tumor necrosis factor-alpha and macrophage inflammatory protein-1 alpha. *J Clin Invest* 1993;**91**:2673–84.

- [10] Hamid Q, Barkans J, Meng Q, et al. Human eosinophils synthesize and secrete interleukin-6, in vitro. *Blood* 1992;**80**:1496–501.
- [11] Weller PF, Rand TH, Barrett T, Elovic A, Wong DT, Finberg RW. Accessory cell function of human eosinophils. HLA-DR-dependent, MHC-restricted antigen-presentation and IL-1 alpha expression. *J Immunol* 1993;**150**:2554–62.
- [12] Wong DT, Weller PF, Galli SJ, et al. Human eosinophils express transforming growth factor alpha. *J Exp Med* 1990;**172**:673–81.
- [13] Wong DTW, Elovic A, Matossian K, et al. Eosinophils From Patients With Blood Eosinophilia Express Transforming Growth Factor β 1. *Blood* 1991;**78**:2702–7.
- [14] Dorta RG, Landman G, Kowalski LP, Lauris JR, Latorre MR, Oliveira DT. Tumour-associated tissue eosinophilia as a prognostic factor in oral squamous cell carcinomas. *Histopathology* 2002;**41**:152–7.
- [15] Hu G, Wang S, Zhong K, et al. Tumor-associated tissue eosinophilia predicts favorable clinical outcome in solid tumors: a meta-analysis. *BMC Cancer* 2020;**20**:454.
- [16] Peurala E, Tuominen M, Loyttyneimi E, Syrjanen S, Rautava J. Eosinophilia is a favorable prognostic marker for oral cavity and lip squamous cell carcinoma. *APMIS* 2018;**126**:201–7.
- [17] Thompson AC, Bradley PJ, Griffin NR. Tumor-associated tissue eosinophilia and long-term prognosis for carcinoma of the larynx. *Am J Surg* 1994;**168**:469–71.
- [18] Alrawi SJ, Tan D, Stoler DL, et al. Tissue eosinophilic infiltration: a useful marker for assessing stromal invasion, survival and locoregional recurrence in head and neck squamous neoplasia. *Cancer J* 2005;**11**:217–25.
- [19] De Paz D, Chang KP, Kao HK, et al. Clinical Implications of Tumor-Associated Tissue Eosinophilia in Tongue Squamous Cell Carcinoma. *Laryngoscope* 2019;**129**:1123–9.
- [20] Oliveira DT, Biassi TP, Faustino SE, Carvalho AL, Landman G, Kowalski LP. Eosinophils may predict occult lymph node metastasis in early oral cancer. *Clin Oral Investig* 2012;**16**:1523–8.
- [21] Tostes Oliveira D, Tjioe KC, Assao A, et al. Tissue Eosinophilia and its Association with Tumoral Invasion of Oral Cancer. *Int J Surg Pathol* 2009;**17**:244–9.
- [22] Messingham KN, Wang JW, Holahan HM, Srikantha R, Aust SC, Fairley JA. Eosinophil localization to the basement membrane zone is autoantibody- and complement-dependent in a human cryosection model of bullous pemphigoid. *Exp Dermatol* 2016;**25**:50–5.
- [23] Hiraguchi Y, Nagao M, Hosoki K, Tokuda R, Fujisawa T. Neutrophil Proteases Activate Eosinophil Function in vitro. *Int Arch Allergy Immunol* 2008;**146**(Suppl 1):16–21.
- [24] Yang MH, Chang SY, Chiou SH, et al. Overexpression of NBS1 induces epithelial-mesenchymal transition and co-expression of NBS1 and Snail predicts metastasis of head and neck cancer. *Oncogene* 2007;**26**:1459–67.
- [25] Lee CC, Lin JC, Hwang WL, et al. Macrophage-secreted interleukin-35 regulates cancer cell plasticity to facilitate metastatic colonization. *Nat Commun* 2018;**9**:3763.
- [26] Li CF, Chen JY, Ho YH, et al. Snail-induced claudin-11 prompts collective migration for tumour progression. *Nat Cell Biol* 2019;**21**:251–62.
- [27] Liberzon A, Birger C, Thorvaldsdottir H, Ghandi M, Mesirov JP, Tamayo P. The Molecular Signatures Database (MSigDB) hallmark gene set collection. *Cell Syst* 2015;**1**:417–25.
- [28] Cancer Genome Atlas N. Comprehensive genomic characterization of head and neck squamous cell carcinomas. *Nature* 2015;**517**:576–82.
- [29] Li T, Fu J, Zeng Z, et al. TIMER2.0 for analysis of tumor-infiltrating immune cells. *Nucleic Acids Res* 2020;**48**:W509–14.
- [30] Ling Z, Yang X, Chen X, Xia J, Cheng B, Tao X. CCL2 promotes cell migration by inducing epithelial-mesenchymal transition in oral squamous cell carcinoma. *J Oral Pathol Med* 2019;**48**:477–82.
- [31] Grivennikov SI, Greten FR, Karin M. Immunity, inflammation, and cancer. *Cell* 2010;**140**:883–99.
- [32] Baram D, Vaday GG, Salamon P, Drucker I, Hershkoviz R, Mekori YA. Human mast cells release metalloproteinase-9 on contact with activated T cells: juxtacrine regulation by TNF-alpha. *J Immunol* 2001;**167**:4008–16.
- [33] Fang KC, Wolters PJ, Steinhoff M, Bidgol A, Blount JL, Caughey GH. Mast Cell Expression of Gelatinases A and B Is Regulated by kit Ligand and TGF- β . *J Immunol* 1999;**162**:5528–35.
- [34] Schwingshackl A, Duszyk M, Brown N, Moqbel R. Human eosinophils release matrix metalloproteinase-9 on stimulation with TNF- α . *J Allergy Clin Immunol* 1999;**104**:983–90.
- [35] Tanaka A, Arai K, Kitamura Y, Matsuda H. Matrix Metalloproteinase-9 Production, a Newly Identified Function of Mast Cell Progenitors, Is Downregulated by c-kit Receptor Activation. *Blood* 1999;**94**:2390–5.
- [36] Okada S, Kita H, George TJ, Gleich GJ, Leiferman KM. Migration of Eosinophils through Basement Membrane Components In Vitro: Role of Matrix Metalloproteinase-9. *Am J Respir Cell Mol Biol* 1997;**17**:519–28.
- [37] Zaynagetdinov R, Sherrill TP, Gleaves LA, et al. Interleukin-5 Facilitates Lung Metastasis by Modulating the Immune Microenvironment. *Cancer Res* 2015;**75**:1624–34.
- [38] Panagopoulos V, Leach DA, Zinonos I, et al. Inflammatory peroxidases promote breast cancer progression in mice via regulation of the tumour microenvironment. *Int J Oncol* 2017;**50**:1191–200.
- [39] Li F, Du X, Lan F, et al. Eosinophilic inflammation promotes CCL6-dependent metastatic tumor growth. *Sci Adv* 2021;**7**.
- [40] Kitamura T, Qian B-Z, Soong D, et al. CCL2-induced chemokine cascade promotes breast cancer metastasis by enhancing retention of metastasis-associated macrophages. *J Exp Med* 2015;**212**:1043–59.
- [41] Zhang YJ, Rutledge BJ, Rollins BJ. Structure/activity analysis of human monocyte chemoattractant protein-1 (MCP-1) by mutagenesis. Identification of a mutated protein that inhibits MCP-1-mediated monocyte chemotaxis. *J Biol Chem* 1994;**269**:15918–24.
- [42] Horiuchi T, Weller PF. Expression of vascular endothelial growth factor by human eosinophils: upregulation by granulocyte macrophage colony-stimulating factor and interleukin-5. *Am J Respir Cell Mol Biol* 1997;**17**:70–7.
- [43] Hoshino M, Takahashi M, Aoike N. Expression of vascular endothelial growth factor, basic fibroblast growth factor, and angiogenin immunoreactivity in asthmatic airways and its relationship to angiogenesis. *J Allergy Clin Immunol* 2001;**107**:295–301.
- [44] Kita H, Ohnishi T, Okubo Y, Weiler D, Abrams JS, Gleich GJ. Granulocyte/macrophage colony-stimulating factor and interleukin 3 release from human peripheral blood eosinophils and neutrophils. *J Exp Med* 1991;**174**:745–8.
- [45] Puxeddu I, Alian A, Piliponsky AM, Ribatti D, Panet A, Levi-Schaffer F. Human peripheral blood eosinophils induce angiogenesis. *Int J Biochem Cell Biol* 2005;**37**:628–36.
- [46] Yousefi S, Hemmann S, Weber M, et al. IL-8 is expressed by human peripheral blood eosinophils. Evidence for increased secretion in asthma. *J Immunol* 1995;**154**:5481–90.